

Magnetism of two-dimensional triangular nanoflake-based kagome lattices

This article has been downloaded from IOPscience. Please scroll down to see the full text article.

2012 New J. Phys. 14 033043

(<http://iopscience.iop.org/1367-2630/14/3/033043>)

View [the table of contents for this issue](#), or go to the [journal homepage](#) for more

Download details:

IP Address: 128.172.52.254

The article was downloaded on 11/07/2012 at 15:28

Please note that [terms and conditions apply](#).

Magnetism of two-dimensional triangular nanoflake-based kagome lattices

Xiaowei Li¹, Jian Zhou², Qian Wang^{1,3,6}, Xiaoshuang Chen⁴,
Y Kawazoe⁵ and P Jena³

¹ HEDPS, Center for Applied Physics and Technology, College of Engineering, Peking University, Beijing 100871, People's Republic of China

² Department of Material Science and Engineering, College of Engineering, Peking University, Beijing 100871, People's Republic of China

³ Department of Physics, Virginia Commonwealth University, Richmond, VI 23284, USA

⁴ Institute of Technical Physics, Chinese Academy of Science, Shanghai 200083, People's Republic of China

⁵ Institute for Material Research, Tohoku University, Sendai 980-8577, Japan
E-mail: qianwang2@pku.edu.cn

New Journal of Physics **14** (2012) 033043 (11pp)

Received 7 December 2011

Published 30 March 2012

Online at <http://www.njp.org/>

doi:10.1088/1367-2630/14/3/033043

Abstract. We report a new method for the design of kagome lattices using zigzag-edged triangular graphene nanoflakes (TGFs) linked with B, C, N or O atoms. Using spin-polarized density functional theory we show that the electronic and magnetic properties of the designed kagome lattices can be modulated by changing their size and the linking atoms. The antiferromagnetic coupling between the two directly linked TGFs becomes ferromagnetic coupling when B, C or N is used as the linking atoms, but not for O atom linking. All the designed structures are semiconductors which can be synthesized from graphene atomic sheets by using electron etching and block copolymer lithography techniques. This study is a good example of how mathematical models can be used to construct magnetic nanostructures involving only s, p elements.

⁶ Author to whom any correspondence should be addressed.

Contents

1. Introduction	2
2. Theoretical procedure	3
3. Results and discussion	3
4. Conclusions	9
Acknowledgments	10
References	10

1. Introduction

Spintronics that exploits the electron's spin degree of freedom has been a robust and challenging field of research over the last decade owing to its technological importance for new electronic devices. An ideal spintronics material should possess high spin polarization, long spin relaxation time, weak spin-orbit coupling and ferromagnetic (FM) ordering at room temperature. Past studies on spintronics materials have mainly focused on transition metal impurity-doped GaN and ZnO where the magnetism is due to d-electrons [1, 2]. However, these materials have the disadvantages of clustering of impurity atoms [1], strong spin-orbit interaction and small spin relaxation time. Consequently, attention has now shifted to magnetic semiconductors where the magnetism is associated with s-, p-electrons. These materials have the advantage of low spin-orbit coupling, weak hyperfine interaction and no clustering. Among s, p elements, graphene-based structures are a natural choice. These include graphene nanoribbons (GNRs) and triangular graphene nanoflakes (TGFs), which can be fabricated by cutting graphene sheets using electron beam irradiation and etching techniques [3, 4], or the atomic force microscope-based nanorobot [5]. In GNRs, although the zigzag edge states are FM, the opposite edges are coupled antiferromagnetically due to the anti-pattern rule, resulting in zero net magnetic moment [6–8]. However, in the TGFs the magnetic coupling between the zigzag edges is FM [9–15], and the non-equivalent sublattices A and B lead to a size-dependent magnetic moment of $(N - 1) \mu_B$, where N is the number of hexagons along one edge of the TGF. Compared to GNRs, the zigzag-edged TGFs therefore have some advantages in the synthesis of magnetic materials. In addition, unlike conventional magnetic materials where magnetism is due to d- or f-electrons, magnetism in the TGFs originates from the p-electrons, displaying weak spin-orbit coupling and low hyperfine interaction of the electron spins with the carbon nuclei, which are the main channels of relaxation and decoherence of electron spins [16]. Recent studies have focused on the assembling of TGFs by finding suitable linkers so as to promote FM ordering [17]. In this paper, we show that new graphene-based magnetic materials can be created by using an old mathematical model known as the kagome lattice.

A kagome lattice, composed of interlaced triangles in a two-dimensional (2D) pattern, is a well-known mathematical model widely used in the study of frustrated magnetism [18]. Although called a lattice, it is more closely related to tri-hexagonal tiling. A large number of research works in past years have been devoted to using this model to design and synthesize materials. For example, Ramirez *et al* [19] studied $\text{SrCr}_8\text{Ga}_4\text{O}_{19}$ where Cr ions form a kagome lattice with a high Curie-Weiss temperature of 515 K. Schweika *et al* [20] synthesized layered kagome materials consisting of $\text{Y}_{0.5}\text{Ca}_{0.5}\text{BaCo}_4\text{O}_7$, which exhibits a high Curie-Weiss temperature of 2200 K. Aidoudi *et al* [21] fabricated an inorganic-organic hybrid kagome

structure containing V ions, which displays antiferromagnetic (AFM) behavior. Currently, a new direction in synthesizing kagome lattices on the surface is by means of metal–organic coordination or supramolecular self-assembly of specific molecules. For instance, Mao *et al* [22] deposited Fe-phthalocyanine (FePc) molecules on highly ordered graphene monolayer (MG) supported on a Ru (0001) substrate that mimics a well-assembled kagome lattice. Wang *et al* [23] constructed a kagome lattice from Co ions and azide ligands showing antiferromagnetism. Colloidal kagome lattices using tri-block Janus spheres containing sulfate polystyrene with hydrophobic poles synthesized by Chen *et al* [24] showed no magnetism. Until recently, all existing methods for the synthesis of kagome lattices have been very complicated. Only transition metal ions have been used to induce magnetism, and the substrate surface has to be carefully chosen for assembling 2D kagome lattices. Thus, the question arises: can we find a simple route to achieve a 2D magnetic kagome lattice without using *any* metal ions? In this paper, a novel approach is provided for constructing a 2D periodic magnetic kagome lattice by using magnetic TGFs as the building blocks because of their excellent geometric shape and intrinsic magnetism. Using spin-polarized density functional theory (DFT) combined with Monte Carlo simulations, we have systematically studied the geometry, electronic structure and magnetic properties of TGF-based 2D kagome lattices.

2. Theoretical procedure

A unit cell representing a 2D periodic structure has been generated by inserting two zigzag-edged TGFs into the nearest triangles of kagome lattices and linking these with four different atoms M ($M = \text{B, C, N and O}$, respectively). A vacuum space of 12 Å in the non-periodic direction is used to avoid interaction between the two neighboring images. Here, the number N of the hexagons along one edge of the TGF_N is used to define the size of a TGF_N . To study the size dependence, we have changed the size of TGF_N s from $N = 2$ to 4 and constructed different size 2D kagome lattices, labeled as $\text{TGF}_N\text{-M-TGF}_N$. The schematic structures of perfect and deformed kagome lattices with $N = 3$ are shown in figures 1 and 2, respectively. Calculations were performed by using spin-polarized DFT and the Vienna *ab initio* Simulation Package (VASP) code [25]. Generalized gradient approximation with the Perdew–Burke–Ernzerhof form was used to treat the exchange and correlation potentials [26]. The Brillouin zones are represented by the Monkhorst–Pack special k -point meshes of $n \times n \times 1$ with $n = 7, 5$ and 3 for the unit cells with size N of 2, 3 and 4, respectively. The energy cutoff was set to 400 eV. All the atoms were fully relaxed using a conjugate-gradient algorithm until the variations of energy and force between two steps were less than 0.01 meV and $0.004 \text{ eV \AA}^{-1}$, respectively. In order to examine the magnetic behavior of these periodic frameworks at finite temperatures, we carried out Monte Carlo simulations for a (10×10) supercell system by using the Ising model. The simulations lasted for 1×10^5 loops in order to analyze the data, and in each loop all the magnetic moments of the TGFs and the linking atoms were allowed to change.

3. Results and discussion

We first studied the magnetic coupling between the two zigzag-edged isolated TGF_N s ($N = 2, 3$ and 4). In agreement with previous calculations [17] we found that the two TGF_N s are coupled antiferromagnetically when they are directly connected, regardless of the size N of TGF_N s. Stimulated by the pioneering work of Rao and Jena [1] and Tono *et al* [27] on tuning

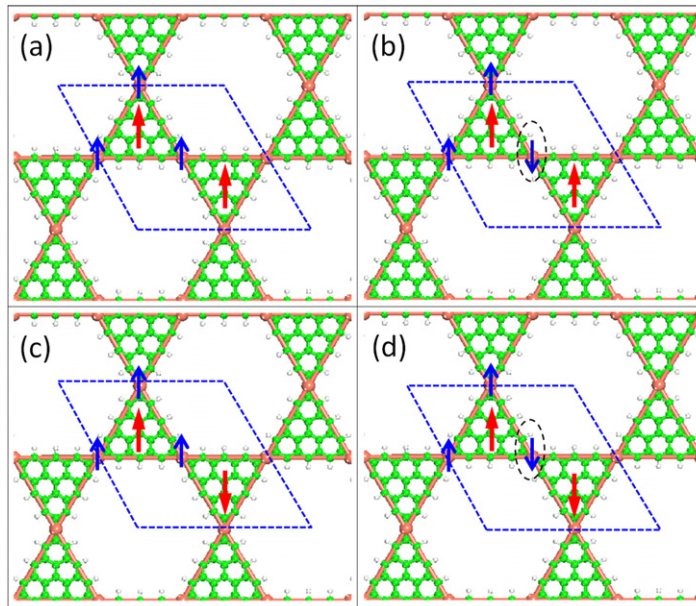


Figure 1. Schematic structures of the 2D TGF₃S-based kagome lattice with different spin coupling configurations. (a) FM coupling between the TGF₃S (red arrows) with the FM spin alignment of kagome sites (blue arrows). (b) FM coupling between the TGF₃S with the AFM spin alignment of the kagome site. (c) AFM coupling between the TGF₃S with the FM spin alignment of the kagome sites. (d) AFM coupling between the TGF₃S with the AFM kagome sites. The green, orange and white balls correspond to C atoms, kagome sites and H atoms, respectively.

the magnetic coupling in clusters by using 2p electrons of N and O atoms, respectively, we introduced a single atom, M (M = B, C, N and O), between the two TGF_Ns to mediate their magnetic coupling. We refer to this as the 0D structure. It is interesting to see that the AFM coupling between the two TGF_Ns turns into FM when they are connected by a single B, C or N atom, while the AFM coupling configuration still exists when an O atom is introduced between them. For instance, the FM configuration is found to be lower in energy by 0.20, 0.18, and 0.15 eV than the AFM one for the systems composed of two TGF₃s linked by a single B, C or N atom, respectively. However, the AFM configuration is found to be lower in energy by 0.01 eV than the FM one when one O atom is used as the linker. This indicates that the magnetic coupling between the two TGFs can be changed from AFM to FM by introducing B, C or N atoms. The calculated results for the 0D structures are given in table 1. From their geometries we can see the difference: the centers of two TGFs and the kagome site remain in a straight line when they are linked by a B atom, i.e. the angle θ between the two B–C bonds is 180°. However, when C, N and O atoms are used as the linkers, the corresponding angles change to 146.8°, 131.2° and 132.5°, respectively. From the spin density isosurfaces we can see the similarity: for all the systems the magnetic moment mainly comes from the 2p orbitals of C atoms at the sublattice A sites of the TGFs. The spin density on the C atoms at the sublattice B sites is small and has the opposite spin direction, which results in a net magnetic moment of 5.0, 6.0 and 5.0 μ_B for the systems containing B, C and N atoms, respectively. This can be understood from Lieb's

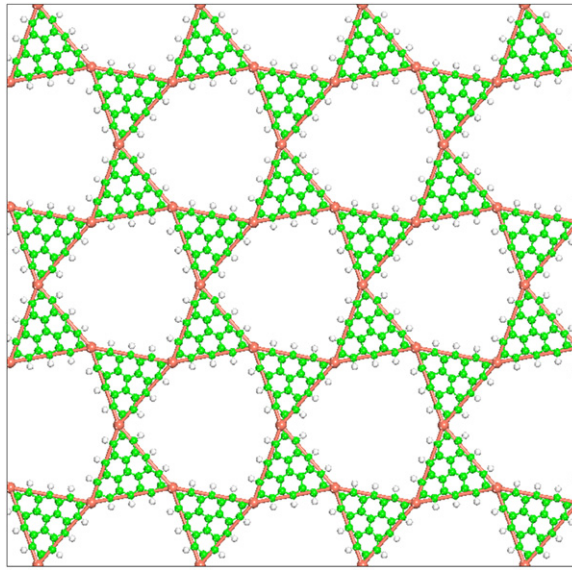


Figure 2. Schematic structure of the 2D deformed kagome lattice composed of the TGF_3 s and the linking atoms M ($M = \text{C}, \text{N}$ and O) on the kagome sites.

theorem [28]: defining hydrogenated carbon atoms at the edges as A sites and their neighboring sites as B sites, the numbers of A and B sites in the TGF_N are given by $N_A = (N^2 + 5N)/2$ and $N_B = (N^2 + 3N + 2)/2$, respectively. The difference between the numbers of carbon atoms at A and B sites is: $(N_A - N_B) = (N - 1)$. Thus, each zigzag-edged TGF_3 carries a magnetic moment of $2.0 \mu_B$. For the linkers of B, C and N atoms, they are sp hybridized in the assembled structures and have different numbers of 2p valence electrons, making each B, C and N atom contribute 1.0, 2.0 and 1.0 μ_B , respectively. Therefore, the total moments of the systems composed of the two TGF_3 s and a single atom M ($M = \text{B}, \text{C}$ and N) are 5.0, 6.0 and 5.0 μ_B , respectively. If the O atom is used as the linker, the two TNF_N s, however, still prefer AFM with a total moment of 0.0 μ_B .

Based on the above study of two isolated TGF_N s linked by B, C, N and O atoms, we then construct a kagome lattice by forming a 2D periodic structure with these 0D structures as building blocks. The initial schematic structure of the TGF_N s-based kagome lattice is plotted in figure 1, where each unit cell of the kagome lattice contains the two TGF_N s and three linking M ($M = \text{B}, \text{C}, \text{N}$ and O) atoms. Four different spin coupling configurations are considered to determine the preferred magnetic state. For each structure of $\text{TGF}_N\text{-M-TGF}_N$ with $N = 2, 3$ and 4, the total energies corresponding to the four spin configurations were calculated. The energy difference ΔE between the FM configuration, as shown in figure 1(a), and the AFM configurations, as shown in figures 1(b)–(d), is defined as $\Delta E = E_{\text{AFM}} - E_{\text{FM}}$. Geometry optimizations were carried out for all the above configurations. The optimized geometries can be divided into two kinds: one is the TGF_N s-based perfect kagome lattice, as shown in figure 1. The other is the deformed kagome lattice, as shown in figure 2. We note that the results for the 0D systems are also valid in their corresponding 2D structures. We find that the centers of two TGF_N s and the kagome site in the unit cell of the 2D $\text{TGF}_N\text{-B-TGF}_N$ ($N = 2, 3$ and 4) structures always remain on a straight line. The structures of $\text{TGF}_N\text{-M-TGF}_N$ ($M = \text{C}, \text{N}$ and O), on the other hand, bend at the kagome sites, as shown in figure 2. Both the angle θ

Table 1. Spin density isosurface; the angle θ consisted of the linking atom M and its nearest two C atoms, magnetic moments M and energy difference ΔE between the FM and AFM states ($\Delta E = E_{\text{AFM}} - E_{\text{FM}}$) for the 0D structures of $\text{TGF}_3\text{-M-TGF}_3$ (M = B, C, N and O).

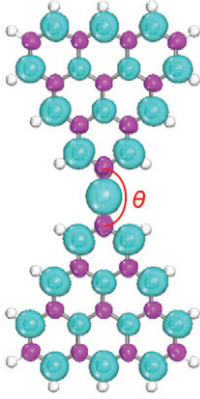
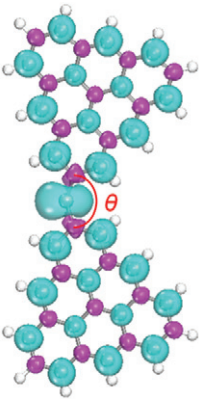
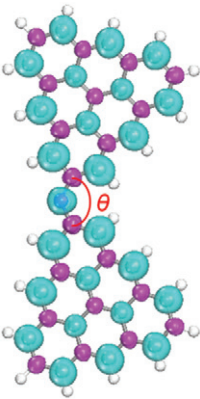
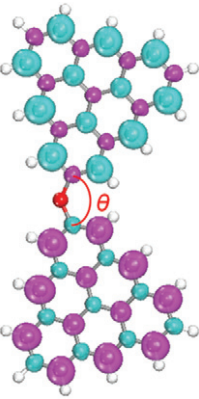
0D structure:	$\text{TGF}_3\text{-B-TGF}_3$	$\text{TGF}_3\text{-C-TGF}_3$	$\text{TGF}_3\text{-N-TGF}_3$	$\text{TGF}_3\text{-O-TGF}_3$
Spin density:				
θ (deg)	180.00	146.77	131.23	132.49
ΔE (eV)	0.20	0.18	0.15	-0.01
M (μ_B)	5.00	6.00	5.00	0.00

Table 2. The calculated angle θ between the linking atom and its nearest two C atoms, the lattice parameter L , the magnetic moment M per unit cell and the energy differences ΔE between the FM (as shown in figure 1(a)) and the AFM configurations ($\Delta E = E_{\text{AFM}} - E_{\text{FM}}$) (as shown in figures 1(b)–(d)) for the 2D periodic kagome structures.

2D structure:	$\text{TGF}_3\text{-B-TGF}_3$	$\text{TGF}_3\text{-C-TGF}_3$	$\text{TGF}_3\text{-N-TGF}_3$	$\text{TGF}_3\text{-O-TGF}_3$
θ (deg)	180.00	155.39	134.22	133.69
L (\AA)	19.98	19.33	18.94	18.75
$\Delta E^{(b)}$ (eV)	–	0.24	–	0.00
$\Delta E^{(c)}$ (eV)	0.40	0.56	0.37	-0.01
$\Delta E^{(d)}$ (eV)	0.24	0.58	0.28	-0.01
M (μ_B)	7.00	10.00	7.00	0.00

and lattice parameter L decrease with increasing valence electrons of the linking atoms from B, C, N to O. This trend is not affected by the size N of the TGF_N s. The calculated geometric parameters, energy difference between the FM and AFM coupling configurations and the total magnetic moment per unit cell of the 2D structures of $\text{TGF}_3\text{-M-TGF}_3$ (M = B, C, N and O) are given in table 2.

All the constructed 2D periodic $\text{TGF}_3\text{-M-TGF}_3$ with M = B, C and N structures are found to have FM ground states. Among them, the $\text{TGF}_3\text{-C-TGF}_3$ has the largest energy difference ΔE_C between the FM and AFM states, indicating that the C atom is more effective in mediating the magnetic coupling between the TGFs, as compared to B, N and O atoms, and the system

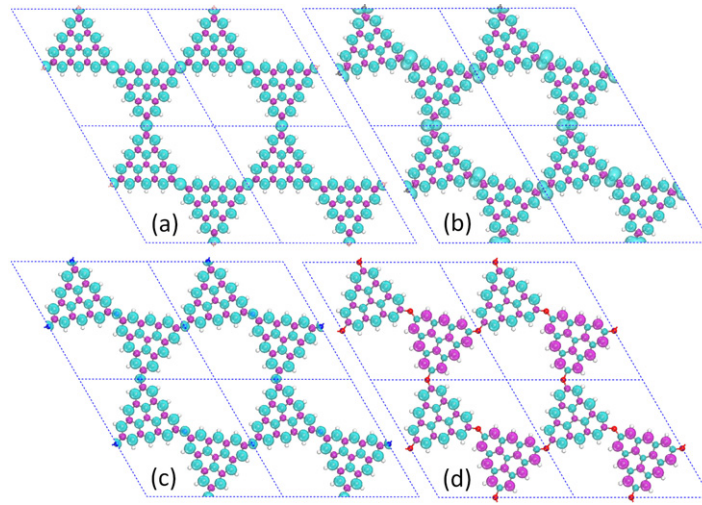


Figure 3. Spin density isosurface with the value of $0.02 \mu_B \text{ \AA}^{-3}$ of the 2D (a) $\text{TGF}_3\text{-B-TGF}_3$ in the FM, (b) $\text{TGF}_3\text{-C-TGF}_3$ in the FM, (c) $\text{TGF}_3\text{-N-TGF}_3$ in the FM and (d) $\text{TGF}_3\text{-O-TGF}_3$ in the AFM states, having 2×2 unit cells.

clearly prefers FM coupling as the AFM states lead to higher total energy, as shown in table 2, $\Delta E_C^{(d)} > \Delta E_C^{(c)} > \Delta E_C^{(b)} > 0.0 \text{ eV}$. We note that the spin direction of the linking atom M (M = B and N) at the kagome site in the coupling configuration, as shown in figure 1(b), flips to the same direction as its nearest neighbors (TGF_N s) upon geometry optimization, namely the AFM configuration of figure 1(b) turns into FM coupling, as shown in figure 1(a). We note that the difference between $\Delta E_M^{(c)}$ and $\Delta E_M^{(d)}$ for all the constructed FM 2D periodic structures decreases with an increase in size N . This is because the coupling between the TGF_N s becomes weaker when their size gets larger and the spin direction of the linking atom plays a relatively weaker role in mediating the coupling. Therefore, the configurations (c) and (d) become energetically nearly degenerate when $N = 4$. For the assembled 2D $\text{TGF}_N\text{-O-TGF}_N$ ($N = 2, 3$ and 4) structures, the AFM configuration, as shown in figure 1(c), is found to be lower in energy than the FM one (see figure 1(a)). Taking $N = 3$ as an example, the energy of the AFM ground state is lower than that of the FM state by 10 meV; this energy difference is small and in view of the accuracy of DFT methods, one may argue that the AFM and FM states are nearly degenerate. The configurations of figures 1(a) and (b), and figures 1(c) and (d), respectively, are nearly degenerate. This indicates that the O atom does not play any role in switching the magnetic coupling between the TGFs. The total magnetic moment of the assembled systems is found to depend on the size of TGF_N s and the linking atom M. For example, for the 2D $\text{TGF}_3\text{-M-TGF}_3$ structures with M = B, C, N and O, the total moments of the ground states are calculated to be 7.0, 10.0, 7.0 and 0.0 μ_B per unit cell, respectively. This is because each unit cell contains two of the TGF_3 s and the three linking atoms. Similar to the 0D systems, each TGF_3 contributes a moment of 2.0 μ_B , and each B, C, N and O atom has a moment of 1.0, 2.0, 1.0 and 0.0 μ_B , respectively.

The spin density isosurfaces of the 2D $\text{TGF}_3\text{-M-TGF}_3$ structures with M = B, C, N and O are plotted in figure 3. As compared to the results of 0D structures in table 1, it is interesting to see that the increasing dimension does not affect the distribution of electron spins. The band structures and partial density of states (PDOS), as shown in figure 4, indicate that all the 2D

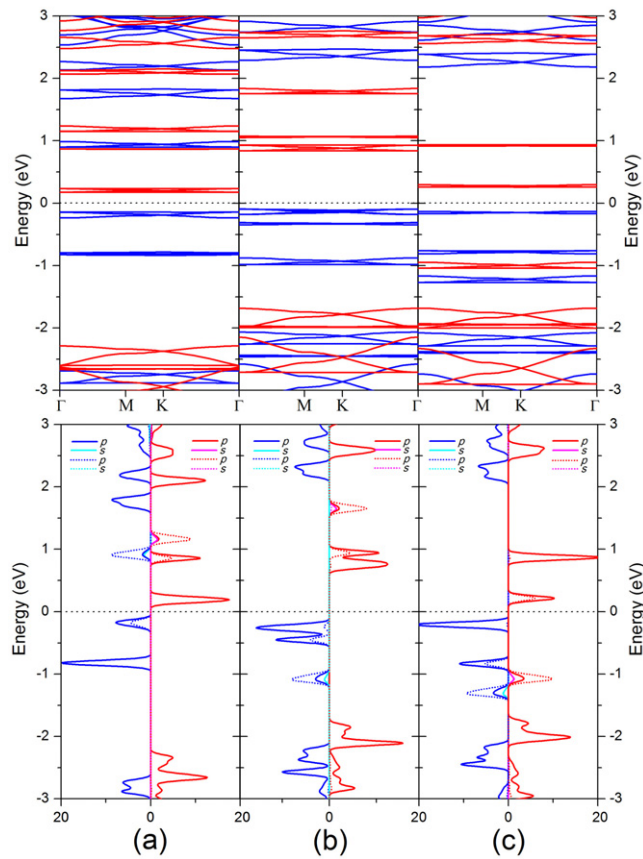


Figure 4. Spin band structures (top) and PDOS (bottom) of the assembled 2D structures: (a) $\text{TGF}_3\text{-B-TGF}_3$, (b) $\text{TGF}_3\text{-C-TGF}_3$ and (c) $\text{TGF}_3\text{-N-TGF}_3$. Blue and red lines are for spin-up and spin-down bands, respectively. Solid and dotted lines in the PDOS represent electronic occupations from the atoms in TGF_3 s and kagome sites, respectively.

periodic $\text{TGF}_3\text{-M-TGF}_3$ structures with $M = \text{B, C}$ and N are FM semiconductors. There are 7, 10 and 7 split energy bands near the Fermi surface for the systems with $M = \text{B, C}$ and N , respectively. This results in different magnetic moments of 7.0 , 10.0 and $7.0 \mu_{\text{B}}$ per unit cell, accordingly. The PDOS shows that the split bands are dominated by the 2p orbitals from both the TGF_3 s and kagome sites. However, the contribution from kagome sites of C atoms to the bands near the Fermi level is larger than that from the B and N atoms due to the different numbers of unpaired valence electrons. The $\text{TGF}_3\text{-C-TGF}_3$ has the largest band gap of 0.93 eV , while the $\text{TGF}_3\text{-B-TGF}_3$ and $\text{TGF}_3\text{-N-TGF}_3$ have smaller band gaps of 0.32 and 0.39 eV , respectively. Therefore, the different band structures of the 2D $\text{TGF}_N\text{-M-TGF}_N$ for $M = \text{B, C}$ and N could be used to identify their geometric structures.

We now carry out Monte Carlo simulations to investigate the magnetic behavior at finite temperatures. In order to calculate the energies for different possible magnetic configurations, we use the Ising model Hamiltonian, $H = - \sum_{\langle i,j \rangle} J_{ij} s_i s_j$, where i and j represent two nearest neighbor magnetic sites, namely the linking atoms and the TGF_N s. In each case, the exchange parameter J can be derived from the energy difference between the FM and AFM states. The

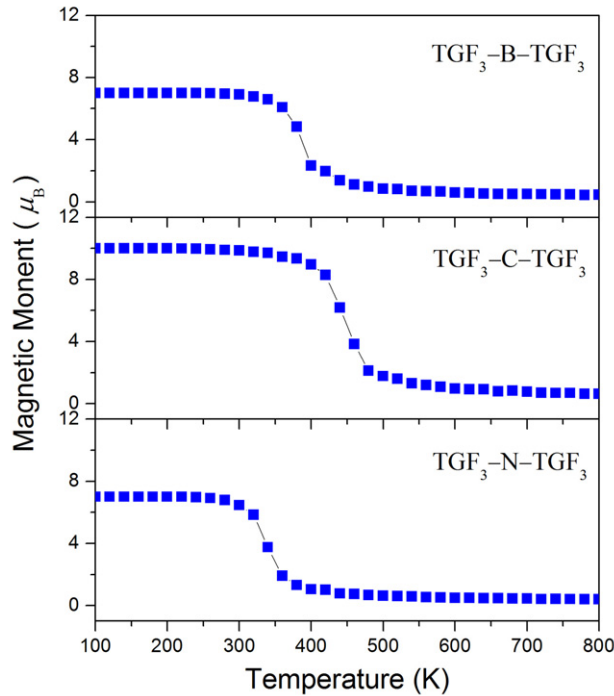


Figure 5. Variation of magnetization per unit cell with temperature of the 2D periodic TGF₃-B-TGF₃, TGF₃-C-TGF₃ and TGF₃-N-TGF₃ structures.

J of the 2D periodic structures of TGF₃-B-TGF₃, TGF₃-C-TGF₃ and TGF₃-N-TGF₃ are calculated to be 34, 23 and 30 meV, respectively. We plot the variation of average magnetic moment per unit cell of the TGF₃-M-TGF₃ (M = B, C and N) with respect to temperature in figure 5. We see that the magnetic moment remains in the high-spin state in the low-temperature range for all the structures and then drops to near zero at the Curie temperature. The corresponding Curie temperatures of the 2D TGF₃-M-TGF₃ structures with M = B, C and N are found to be about 400, 460 and 340 K, respectively. These values indicate that the ferromagnetism that we observed in these TGFs-based kagome lattices can be detected at room temperature. Thus, the designer 2D FM kagome lattices may have advantages over the well-known dilute magnetic semiconductors in the applications of spintronic materials.

4. Conclusions

We present a first-principles study of the geometry and electronic and magnetic properties of TGF_N-based kagome lattices. We show that a magnetic kagome lattice can be achieved by using zigzag-edged TGFs as building blocks and B, C and N atoms as linkers at the kagome sites. B, C and N atoms play an important role in mediating ferromagnetism. Further, their FM coupling strength can be tuned by changing the size of TGF_Ns and the linking atoms. The long-range ferromagnetism together with the ideal Curie temperature calculated by the MC simulations, and the homogeneous porosity makes the TGF_N-based magnetic kagome structures promising for many potential applications. We hope that our work will stimulate experimental studies.

Acknowledgments

This work was supported by grants from the National Natural Science Foundation of China (grant no. NSFC-11174014) and the National Grand Fundamental Research 973 Program of China (grant no. 2012CB921404) and from the US Department of Energy. The authors thank the staff of the Center for Computational Materials Science, Institute for Materials Research, Tohoku University (Japan) for their continuous support of the HITACH SR11000 supercomputing facility.

References

- [1] Rao B K and Jena P 2002 Giant magnetic moments of nitrogen-doped Mn clusters and their relevance to ferromagnetism in Mn-doped GaN *Phys. Rev. Lett.* **89** 185504
- [2] Sharma P, Gupta A, Rao K V, Owens F J, Sharma R, Ahuja R, Guillen J M O, Johansson B and Gehring G A 2003 Ferromagnetism above room temperature in bulk and transparent thin films of Mn-doped ZnO *Nature Mater.* **2** 673–7
- [3] Jin C, Lan H, Peng L, Suenaga K and Iijima S 2009 Deriving carbon atomic chains from graphene *Phys. Rev. Lett.* **102** 205501
- [4] Chuvilin A, Meyer J C, Algara-Siller G and Kaiser U 2009 From graphene constrictions to single carbon chains *New J. Phys.* **11** 083019
- [5] Zhang Y, Liu L Q, Xi N, Wang Y C and Dong Z L 2010 Cutting graphene using an atomic force microscope based nanorobot *Proc. 10th IEEE Int. Conf. on Nanotechnology and Joint Symp. with Nano Korea KINTEX (IEEE-NANO 2010)* pp 639–44
- [6] Lee H, Son Y-W, Park N, Han S and Yu J 2005 Magnetic ordering at the edges of graphitic fragments: magnetic tail interactions between the edge-localized states *Phys. Rev. B* **72** 174431
- [7] Gunlyckea D, Li J, Mintmire J W and White C T 2007 Altering low-bias transport in zigzag-edge graphene nanostrips with edge chemistry *Appl. Phys. Lett.* **91** 112108
- [8] Şahin H and Senger R T 2008 First-principles calculations of spin-dependent conductance of graphene flakes *Phys. Rev. B* **78** 205423
- [9] Şahin H, Senger R T and Ciraci S 2010 Spintronic properties of zigzag-edged triangular graphene flakes *J. Appl. Phys.* **108** 074301
- [10] Wang W L, Meng S and Kaxiras E 2008 Graphene nano flakes with large spin *Nano Lett.* **8** 241
- [11] Ezawa M 2009 Quasiphase transition and many-spin Kondo effects in a graphene nanodisk *Phys. Rev. B* **79** 241407
- [12] Rocha A R, Martins T B, Fazzio A and da Silva A J R 2010 Disorder-based graphene spintronics *Nanotechnology* **21** 345202
- [13] Akola J, Heiskanen H P and Manninen M 2008 Edge-dependent selection rules in magic triangular graphene flakes *Phys. Rev. B* **77** 193410
- [14] Philpott M R, Vukovic S, Kawazoe Y and Lester W A 2010 Edge versus interior in the chemical bonding and magnetism of zigzag-edged triangular graphene molecules *J. Chem. Phys.* **133** 044708
- [15] Potasz P, Güçlü A D, Voznyy O, Folk J A and Hawrylak P 2011 Electronic and magnetic properties of triangular graphene quantum rings *Phys. Rev. B* **83** 174441
- [16] Yazyev O V 2010 Emergence of magnetism in graphene materials and nanostructures *Rep. Prog. Phys.* **73** 056501
- [17] Zhou J, Wang Q, Sun Q and Jena P 2011 Intrinsic ferromagnetism in two-dimensional carbon structures: triangular graphene nanoflakes linked by carbon chains *Phys. Rev. B* **84** 081402
- [18] Syôzi I 1951 Statistics of kagomé lattice *Prog. Theor. Phys.* **6** 306
- [19] Ramirez A P, Espinosa G P and Cooper A S 1990 Strong frustration and dilution-enhanced order in a quasi-2D spin glass *Phys. Rev. Lett.* **64** 2070

- [20] Schweika W, Valldor M and Lemmens P 2007 Approaching the ground state of the kagomé antiferromagnet *Phys. Rev. Lett.* **98** 067201
- [21] Aidoudi F H, Aldous D W, Goff R J, Slawin A M Z, Attfield J P, Morris R E and Lightfoot P 2011 An ionothermally prepared $S = 1/2$ vanadium oxyfluoride kagome lattice *Nature Chem.* **3** 801
- [22] Mao J, Zhang H, Jiang Y, Pan Y, Gao M, Xiao W and Gao H-J 2009 Tunability of supramolecular kagome lattices of magnetic phthalocyanines using graphene-based moiré patterns as templates *J. Am. Chem. Soc.* **131** 14136–7
- [23] Wang X-Y, Wang L, Wang Z-M and Gao S 2006 Solvent-tuned azido-bridged Co^{2+} layers: square, honeycomb, and kagomé *J. Am. Chem. Soc.* **128** 674
- [24] Chen Q, Bae S C and Granick S 2011 Directed self-assembly of a colloidal kagome lattice *Nature* **469** 381
- [25] Kresse G and Furthmüller J 1996 Efficient iterative schemes for *ab initio* total-energy calculations using a plane-wave basis set *Phys. Rev. B* **54** 11169
- [26] Perdew J P, Burke K and Ernzerhof M 1996 Generalized gradient approximation made simple *Phys. Rev. Lett.* **77** 3865
- [27] Tono K, Terasaki A, Ohta T and Kondow T 2003 Chemical control of magnetism: oxidation-induced ferromagnetic spin coupling in the chromium dimer evidenced by photoelectron spectroscopy *Phys. Rev. Lett.* **90** 133402
- [28] Lieb E H 1989 Two theorems on the Hubbard model *Phys. Rev. Lett.* **62** 1201